AFRL-SR-AR-TR-05-

0314

REPORT DOCUMENTATION PAGE

1. REPORT DATE *(DD-MM-YYYY)*	2. REPORT TYPE	3. DATES COVERED *(From - To)*
21/01/2005	FINAL	Jan 2002 - December 2004

4. TITLE AND SUBTITLE
Control of high-speed flows using helium injection

5a. CONTRACT NUMBER

5b. GRANT NUMBER
F49620-02-0124

5c. PROGRAM ELEMENT NUMBER

6. AUTHOR(S)
Alexander J. Smits

Richard B. Miles

5d. PROJECT NUMBER

5e. TASK NUMBER

5f. WORK UNIT NUMBER

7. PERFORMING ORGANIZATION NAME(S) AND ADDRESS(ES)

Princeton University
Nassau Street
Princeton, NJ 08544

8. PERFORMING ORGANIZATION REPORT NUMBER

9. SPONSORING / MONITORING AGENCY NAME(S) AND ADDRESS(ES)
AFOSR
4015 Wilson Boulevard
Room 713
Arlington, VA 22203-1954

10. SPONSOR/MONITOR'S ACRONYM(S)
AFOSR

11. SPONSOR/MONITOR'S REPORT NUMBER(S)

12. DISTRIBUTION / AVAILABILITY STATEMENT

Approved for public release,
distribution unlimited

13. SUPPLEMENTARY NOTES

14. ABSTRACT

Here, we summarize the results of our investigation of means for controlling high-speed flows using helium injection, first demonstrated by Auvity et al., with particular emphasis on the wavefront distortion of light transmitted through the boundary layer. Quantitative estimates of wavefront distortion were obtained, with and without helium injection, and new diagnostic techniques were developed, including a MHz rate Hartmann wavefront sensor. In particular, we demonstrated the ability to capture real-time wavefront data in two dimensions using an ultra-fast Shack-Hartmann sensor in hypersonic and transonic turbulent boundary layers. These measurements are unrivalled in their temporal resolution (2 □s), while providing full dimensional information on the planar field. This capability, and the data in themselves, are vital for making accurate and complete estimates of aero-optic distortion due to boundary layer turbulence in air-borne laser applications, and to assess quantitatively the effectiveness of control methods.

15. SUBJECT TERMS

16. SECURITY CLASSIFICATION OF:			17. LIMITATION OF ABSTRACT	18. NUMBER OF PAGES	19a. NAME OF RESPONSIBLE PERSON
a. REPORT	b. ABSTRACT	c. THIS PAGE			19b. TELEPHONE NUMBER *(include area code)*

20050804006

7-29-05

Standard Form 298 (Rev. 8-98)
Prescribed by ANSI Std. Z39.18

FINAL REPORT

CONTROL OF HIGH-SPEED FLOWS USING HELIUM INJECTION

AFOSR GRANT F-49620-02-1-124

Alexander J. Smits and Richard B. Miles
Department of Mechanical and Aerospace Engineering
Princeton University, Princeton NJ

Abstract

Here, we summarize the results of our investigation of means for controlling high-speed flows using helium injection, first demonstrated by Auvity et al.[1], with particular emphasis on the wavefront distortion of light transmitted through the boundary layer. Quantitative estimates of wavefront distortion were obtained, with and without helium injection, and new diagnostic techniques were developed, including a MHz rate Hartmann wavefront sensor. In particular, we demonstrated the ability to capture real-time wavefront data in two dimensions using an ultra-fast Shack-Hartmann sensor in hypersonic and transonic turbulent boundary layers. These measurements are unrivalled in their temporal resolution (2 μs), while providing full dimensional information on the planar field. This capability, and the data in themselves, are vital for making accurate and complete estimates of aero-optic distortion due to boundary layer turbulence in air-borne laser applications, and to assess quantitatively the effectiveness of control methods.

1. Fundamental Concepts

The index-of-refraction variations that degrade the performance of on-board optical systems for tracking and imaging targets are primarily due to the presence of turbulent free shear layers and turbulent boundary layers, and density discontinuities across shock waves. In directed energy and communication link applications, density fluctuations in the boundary layer cause image break-up and rapidly varying motions, reducing both image and target resolution, and diminishing the power and total energy on target. For tracking applications another important issue is the variation of "bore-sight" error with missile angle-of-attack. Bore-sight error is the difference between the apparent location of the target and its actual location relative to the missile reference frame. As the missile angle-of-attack varies, the apparent location of the target changes because the light rays are bent as they pass through shock waves and through the boundary layer before entering the window.

As the name suggests, aero-optics is the study of the interaction between light and air. More specifically, it is the study and measurement of the distortion of light due to propagation through an index of refraction field which is thin with respect to the imaging (or projecting) aperture. In contrast, atmospheric propagation involves distortion distances much greater than the aperture, and has been studied at some length in the context of ground based

astronomical telescopes. For airborne laser systems, this is called the far field problem. Astronomers are now able to measure and compensate for these distortions in real time, effectively 'de-twinkling' the stars. Aero-optics is concerned with the near field problem, where the distortions are caused by the vehicle flow field itself, and is by comparison at a nascent stage of development.

Aero-optic effects can result in either a gain or loss of information. In the familiar case of schlieren imaging or shadowgraphy, information about the density of the fluid is extracted from the wavefront distortions. On the other hand, if an attempt is made to image through a compressible boundary layer or shock wave, the image will be degraded and information will be lost, that is, the wavefronts are distorted. Measuring this distortion accurately in flows under flight conditions that correspond to practical applications is the primary focus of this proposal.

1.1 Measures of Wavefront Distortion

Both aero-optics and atmospheric propagation arise due to fluctuations in density, □, and the concomitant variations in the index of refraction, n, described by the Gladstone-Dale relation (Jumper and Fitzgerald, 2001),

$$n = 1 + \rho K_{GD}$$

where K_{GD} is the Gladstone-Dale 'constant' which depends on both wavelength and type of fluid. The effect of the index of refraction field is integrated as the light travels through the index of refraction field. The optical path length, OPL, will vary across an initially flat wavefront:

$$OPL(x,z,t) = \int_{y_1}^{y_2} n(x,y,z,t)\,dy \tag{1}$$

In most cases, the optical path difference, OPD is the quantity of interest, not the optical path length:

$$OPD(x,z,t) = OPL(x,z,t) - \overline{OPL(x,z,t)} \tag{2}$$

Fortunately, the OPD is much simpler to measure than the optical path length.

A particularly important figure of merit is the Strehl ratio, defined by

$$SR(t) = \frac{I(t)}{I_0} \tag{3}$$

where I(t) is the maximum light irradiance in the farfield pattern for an aberrated system and I_0 is the maximum light irradiance in the absence of aberrations (Jumper and Fitzgerald, 2001). According to the large-aperture approximation, an estimate for the time-averaged SR for a given optical phase variance, $\sigma^{\square}_{\phi}$, is given by

$$\overline{SR} = \exp(-\sigma_{\phi}^2) \tag{4}$$

The phase variance is essentially the normalized OPD variance:

$$\sigma_\phi^2 \equiv \left(\frac{2\pi OPD_{rms}}{\lambda} \right)^2 \tag{5}$$

where λ is the wavelength of the optical beam. The first design approaches used estimates of the rms degradation to develop systems that could accept these losses (Jumper, 1997).

Note that the maximum light irradiance for a diffraction limited spot is given by

$$I_0 = \frac{P}{\pi Y^2 \lambda^2 / d^2} \tag{6}$$

where P is the laser output power, Y is the propagation distance (that is, the focal length of the optical system) and d is the aperture diameter. The increase of I_0 with increasing λ encourages the use of lasers in the visible spectrum. However, this is based on the unaberrated beam. For an aberrated beam, we see from equations 4 and 5 that the time-averaged SR decreases rapidly with wavelength. Hence, to take advantage of the high irradiance of lasers in the visible, it becomes vital to reduce aero-optical distortions, and increase the time-averaged Strehl ratio.

1.2 Analysis of Turbulent Refractive Index Variations

Reducing the aero-optical distortion requires an understanding of how turbulence contributes to the beam aberration. In a turbulent compressible flow, the flow velocity, density and pressure all vary in space and time. For the refractive index variations, the only important factor is the density variations since the refractive index is proportional to density, according to the Gladstone-Dale relation. The density variations can be estimated from measurements of the velocity fluctuations using Morkovin's (1962) "Strong Reynolds Analogy" (SRA). This analogy states that, as long as the fluctuations in total temperature are small, the fluctuations in temperature are related to the fluctuations in velocity according to:

$$\frac{T'}{\overline{T}} = \frac{(\gamma - 1)}{2} M^2 \frac{u'}{\overline{U}} \tag{7}$$

From the ideal gas relationship, $p = \rho RT$, we have for small fluctuations:

$$\frac{p'}{\overline{p}} = \frac{\rho'}{\overline{\rho}} + \frac{T'}{\overline{T}} \tag{8}$$

When the pressure fluctuations are small, as they are at low Mach numbers, then

$$\frac{\rho'}{\overline{\rho}} = -\frac{(\gamma - 1)}{2} M^2 \frac{u'}{\overline{U}} \tag{9}$$

For air, $\gamma = 1.4$, and so for $M \leq 1$ the relative density fluctuations are at least an order-of-magnitude smaller than the velocity fluctuations. However, the absolute fluctuations are amplified by the mean density, so that their magnitude depend on altitude and Mach number, as illustrated in Table 1. It is clear from experience that even small density fluctuations can have a major effect on the optical transmissibility of boundary layers and free shear layers.

Altitude(ft)	**Mach #**	**ρ'/ρ**	**ρ' (kg/m^3)**
30,000	0.3	0.0009	0.0000372
30,000	0.8	0.0064	0.00265
30,000	1.5	0.0225	0.0093
20,000	1.5	0.0225	0.0142

Table 1: Density fluctuations in a turbulent boundary layer at the point where u'/U = 0.05, according to the SRA.

To study the connection between the turbulent index-of-refraction field, that is, the instantaneous density field of a compressible boundary layer, and its optical transmission characteristics, it is essential to identify how each of the scales of motion affects the transmission quality.

Turbulence in boundary layers or free shear layers produces three principal sources of optical distortion (Gilbert, 1980; Stanek et al. 2003; Levy, Hornstein & Lednicer, 2003). Small-scale turbulence causes a loss of beam contrast, intermediate-scale turbulence causes beam spread and, therefore, image blurring, and large-scale turbulence causes beam jitter. The boundary layer of high-speed aircraft are fully turbulent and thin, and present a short optical path. However, if separation occurs, they can present a long optical path and can be a source of severe optical degradation. The wavefront error due to turbulence can be estimated by (Sutton, 1980):

$$\sigma_\phi^2 = 2G^2 \int_0^L \overline{\rho'^2}(y)\Lambda(y)dy \tag{7}$$

Here, σ_ϕ is the rms wavefront error in micrometers, L is the path through the turbulent region, Λ is the Eulerian integral scale (a measure of the large-scale turbulent motions), and $G = 2\pi K_{GD}/\lambda$. However, as shown by Cicchiello and Jumper (1997), such indirect methods for estimating the time-averaged Strehl ratio been shown to underestimate the far-field effects of the distortion by orders of magnitude. Direct, real-time measurements of the wavefront distortion, and calculation of its far field are therefore essential, particularly in practical flow fields under realistic flow conditions.

The evolution of the spatial variations in the density field are also of considerable interest. As far as the present proposal is concerned, the most interesting results from our earlier studies of the instantaneous density field of high-speed turbulent boundary layers are:

1. That the largest scales of motion (the turbulent "bulges" that are the most prominent features in Figures 1 and 2) can be crudely modeled as regions of reasonably constant higher temperature interspersed with regions of constant lower freestream density, as suggested by Erbland et al. (1998), and
2. That the largest scales evolve very slowly with streamwise distance.

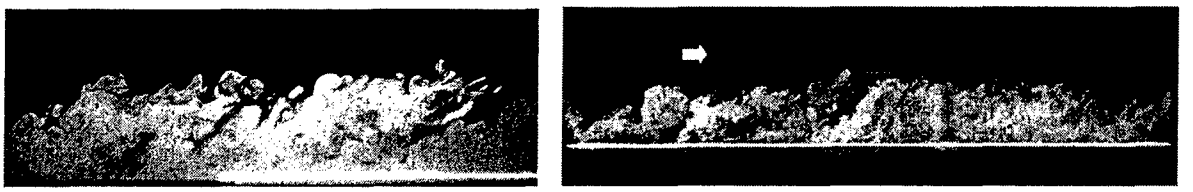

Figure 1: Visualizations of turbulent boundary layers. Flow is from left to right. Left: Subsonic flow. From Falco (1977). Right: Mach 2.9 flow. From Smith & Smits (1995).

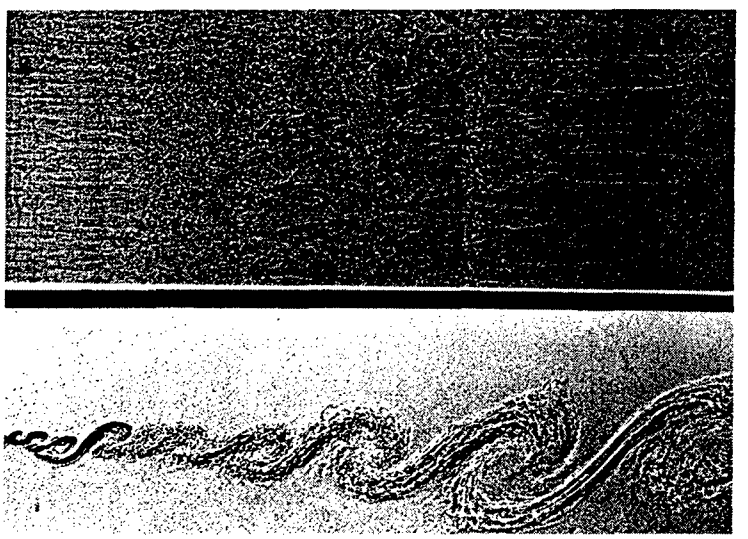

Figure 2: Visualization of a turbulent mixing layer formed between two flows of different density. Flow is from left to right. Top: plan view; Bottom: side view. From Bernal & Roshko (1986).

2. Measuring the Instantaneous OPD Field

To measure the instantaneous optical path differences, Shack-Hartmann sensors have been adapted for aero-optical studies. These sensors consist of an array of small lenslets and a CCD camera. Each lenslet focuses a spot on the CCD array, and typical lenslet arrays provide between 100 and 400 spots in a two-dimensional array. The location of any particular spot depends on the average local wavefront tilt across the lenslet (see Figure 3). Data taken during a run is compared to calibration data, so that the system is relatively

insensitive to misalignment and optical aberrations. The result is an array of slopes that can then be used to reconstruct the original wavefront shape using quadrature or least squares techniques. Spot centroid locations to sub-pixel accuracy using a Gaussian fit, and the phase is recovered by fitting the data to a bi-quadratic surface using singular value decomposition (Southwell 1980, Fitzgerald and Jumper, 1999). See Figure 4.

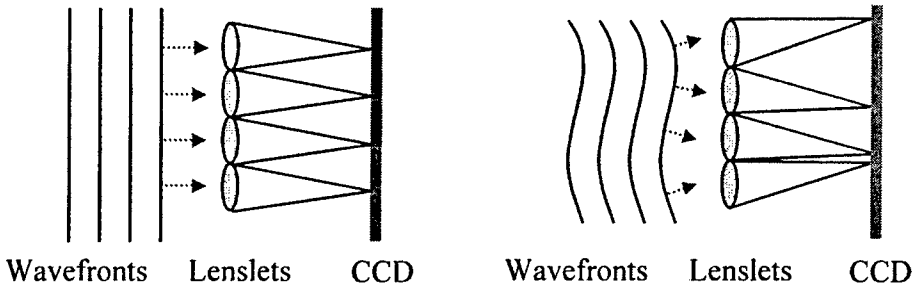

Figure 3: Left: Imaging of planar wavefronts. Right: Imaging of distorted wavefronts..

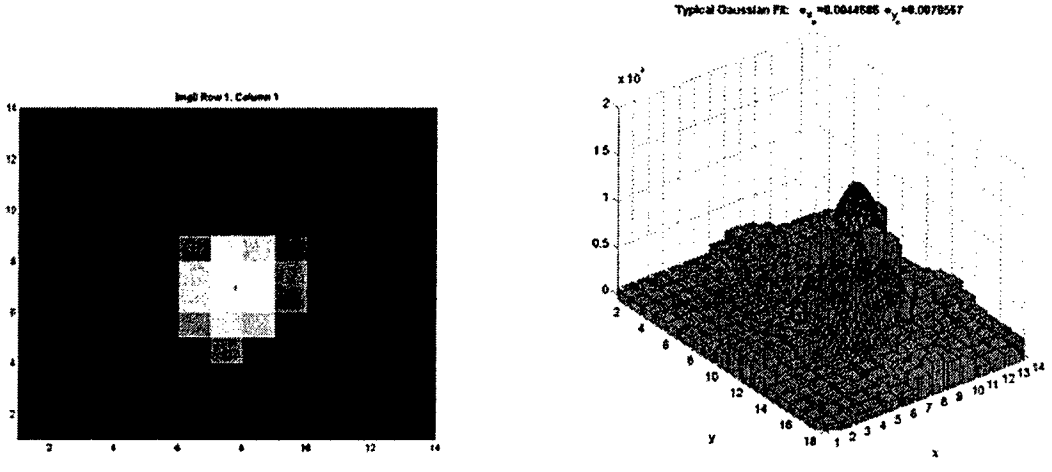

Figure 4: Left: CCD image of a single spot. Right: Gaussian fit to CCD image to find centroid. From Wyckham et al. (2003).

A complementary instrument to a Shack-Hartmann sensor is the so-called Malley probe. A Malley probe is an optical instrument that can measure the time varying OPD at a single point (Gordeyev et al. 2003). The original instrument was described by Malley et al. (1992), and has been developed further by Jumper at Notre Dame (Hugo & Jumper, 1995). It consists of two closely spaced beams (3 to 8 mm apart) aligned, front beam to aft beam, in the streamwise direction. The deflection angles of the beams at the two locations (related to the local OPL) are focused on position sensors that give the spot location as a function of time. First, correlations between the two signals are used to find the phase velocity. Second, by assuming the structures that cause the aberrations convect with the fluid, and that Taylor's hypothesis can be invoked, it is possible to estimate the time-varying OPD. Since the spot centroid can be measured using fast response position sensing devices with response times of order 20 nanoseconds, high

sample rates are possible. Therefore Malley probes can give real-time indications of OPD, something which is not possible at this time using Shack-Hartmann sensors. However, Malley probes are limited to single point measurements, and rely on Taylor's hypothesis to convert time into space to derive the variation of OPD in the streamwise direction. In this respect, it is similar to a hot-wire probe where spatial information may be inferred from the time history by assuming a constant convection velocity. It should be noted that Malley probes cannot give information in the cross-stream direction, and they are expected to become inaccurate under conditions of intense turbulence where Taylor's hypothesis breaks down. In addition, it is possible to use a Shack-Hartmann sensor with a fast camera as a Malley-probe. For a Shack-Hartmann sensor with N lenslets, N-1 Malley probes can be constructed, so it is possible to interpret the Shack-Hartmann data as many different Malley probes if a high frequency response is needed.

Measurement strategies depend on the flow application. Of primary concern is how the length scales in the flow contribute to near-field wavefront distortion The Strehl ratio will depend primarily on the size of the aperture compared to the flow scales (Stanek et al. 2002). For a boundary layer or free shear layer of thickness δ, the largest scales of motion are typically of order $\tilde{\delta}$ Then, if $\delta/A >> 1$, the large-scales will contribute a beam steering component, and smaller scales will contribute to defocusing effects. If δ/A is of order 1, the energy containing range will be important, and the very smallest eddies will create a kind of defocusing (steady image deflection and jitter due to unsteady steering or wavefront tilt). If $\delta/A < 1$, the principal effect is defocusing. For $\delta/A << 1$, all scales will contribute to a kind of defocusing ("large-angle diffractive scattering"). In all cases, there are additional concerns beyond Strehl ratio, such as temporal variations in signal strength, and speckle. For control purposes, in all cases where large scales are important, manipulating the large scales can lead to improvements, as long as the modifications are known and either steadier than the original scales, or of a larger size., since it then possible to use adaptive optics.

The flow geometry is also important, in that it dictates the nature of the shear and boundary layers, and suggests different measurement approaches.

(a) In the flush window case, an attached turbulent boundary layer is present, more or less in equilibrium, so that its structure is reasonably well known. There may or may not be shocks in the medium field
(b) In the recessed window (cavity) case, a separated boundary layer is generated that reattaches on the window at some point (typically 10 or so step heights downstream. For a long window ($L >> \delta$), if the step height is large compared to the boundary layer thickness, the flow structure is reasonably well known (Eaton et al, for example). In this case, we know that the length of the separated zone is very sensitive to disturbances in the upstream boundary layer. If the step height is small compared to the boundary layer thickness, it is seen as a small and rather localized disturbance where the flow recovers relatively quickly (Bradshaw distinguished small perturbations from overwhelming ones on the basis of δ/h). For a short window, we have a cavity flow, so that a shear layer spans the cavity and impinges on the downstream lip, setting up possible resonances. We know that the growth rate of the

separated shear layer is very sensitive to disturbances in the upstream boundary layer (Mehta et al.). Also, we know that the nature of the upstream edge of the cavity affects cavity resonances (e.g., tabs, castellations), as does blowing. Feedback control is being studied by Rowley and Williams.

(c) In the turret case, we have a hemispherical protuberance on the fuselage with the characteristic dimension (say, its height) much larger than the incoming boundary layer thickness. The flow structure is reasonably well known from recent studies by Simpson, and it is extremely complex, in that it contains highly three-dimensional separated shear layers including multiple trailing vortex systems. Simpson has demonstrated that the wake formation and subsequent development displays a high degree of sensitivity to upstream disturbances.

For all these applications, a principal concern is the spatial and temporal resolution of the measurement technique. Whereas Malley probes provide a high frequency response which can be used to estimate the spectral content of the OPD without explicitly providing any spatial information, Shack-Hartmann sensors can be used to study the spatial variation of the OPD in two dimensions simultaneously, and therefore they must be seen as complementary instruments. As already noted, a Shack-Hartmann sensor can always be used as multiple Malley probes as long as a fast camera is available.

3. Mach 8 Results

Our design for the Shack-Hartmann sensor sensor consists of an array of small lenslets and a CCD camera. Each lenslet (diameter of 400 μm and focal length of 71 mm) focuses a spot on the CCD array. Our lenslet array provides a maximum of 20 x 20 spots on the CCD. Spot centroid locations were found to sub-pixel accuracy using a Gaussian fit, and then the phase was recovered by fitting the data to a bi-quadratic surface using singular value decomposition. In all cases, the optical source was the 514 nm (green) component of an argon-ion laser. The camera used in the high Mach number experiments was developed by Princeton Scientific Instruments and is capable of framing rates of up to 500 kHz (or 1 MHz with a 2 μs pause at every fifth frame). This camera uses on-chip memory to produce 30 frame movies (see Figure 5). The camera has 180 x180 pixels and a fill factor of 13.5%, and is described in more detail in Huntley et al. (2000). A similar Shack-Hartmann system with somewhat lower resolution is being independently developed at Ohio State (Thurow et al., 2003). To our knowledge, these two systems are the only ones of their kind, and represent an increase in speed of three orders of magnitude for high resolution wavefront sensors.

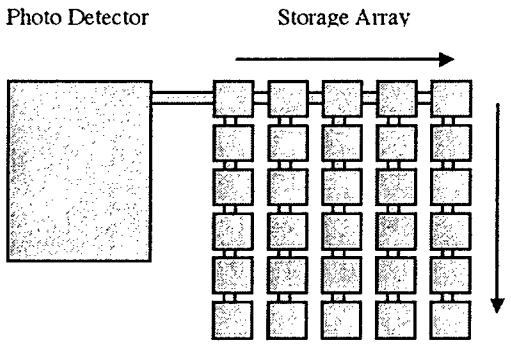

Figure 5: Schematic of one pixel on the PSI fast framing CCD camera.

The PSI fast framing camera has been used extensively at Princeton for the visualization of high speed flows (Huntley et al. 2000; Auvity et al. 2001). Such high framing rates are necessary to resolve the boundary layer motions in time since, characteristically, supersonic boundary layers vary on a microsecond time scale. For the aero-optic application, the 15 ms response time of the mechanical shutter was too slow for our purposes at framing rates greater than 7.8 kHz, so an electronic shutter with an 80 μs response was added to the laser and slaved to the camera's mechanical shutter. In addition, the Shack-Hartmann sensor was improved in terms of its ability to operate at high temperatures, and an error analysis of the system was completed. The sensor was therefore capable of obtaining time-resolved, quantitative measurements of wavefront distortion of known accuracy in a Mach 8 turbulent boundary layer. The effects of helium injection were also studied, since previous experiments by Auvity et al. (2000, 2001) had shown that slot injection of helium in the boundary layer significantly altered the boundary layer structure and seemed to suppress the small-scale high-frequency motions.

All data taken in the high Mach number case were obtained on a flat plate with a stagnation pressure and temperature of 8.2 MPa and 683 K, respectively. No attempt was made to control the temperature of the plate, which started at room temperature. The Reynolds number (Re_x) at the measurement position was approximately 13×10^6.

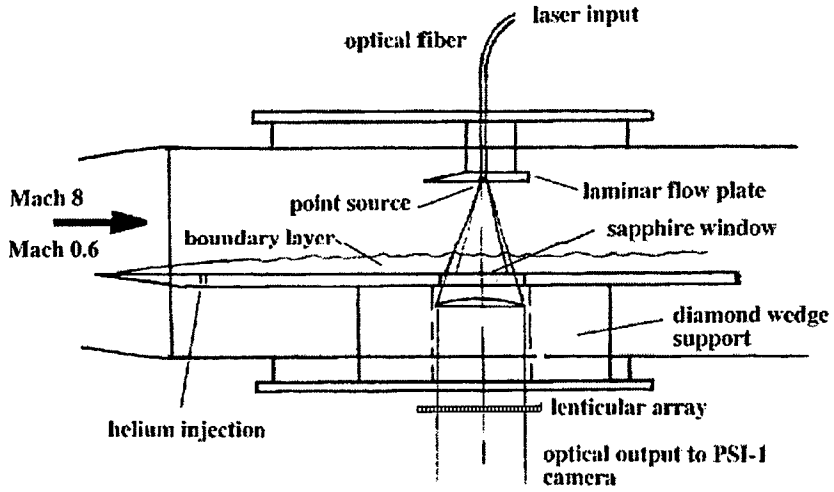

Figure 6: Experimental layout of the test section in Mach 8.0 test facility.

The flat plate model, shown in Figure 6, incorporates a 50 mm diameter window at a distance of 356 mm from the leading edge. There was a 2.4 mm boundary layer trip located 59 mm from the leading edge. The laser is coupled into a single mode optical fibre and then focused through a small hole in a laminar flow plate and into the mean flow. This configuration was chosen to limit distortion due to the tunnel's boundary layer and because it is insensitive to tunnel vibration. The light spreads out conically before passing through the turbulent boundary layer on the flat plate and the window in the model. From there it is collimated by a lens and passes inside the support strut to the Shack-Hartmann sensor. Between the tunnel and the wavefront sensor are two lenses in a 4f configuration. This configuration eliminates diffraction of the signal by exploiting the Fourier transforming property of lenses. By varying the focal length ratio of the two lenses, the beam can also be expanded or contracted to allow a trade-off between sensitivity and spatial sampling frequency. The data presented here were taken using a 2:1 focal length ratio, so that a 1 cm square area on the plate was imaged on the roughly 0.6 mm square CCD chip. This configuration also amplifies the wavefront slopes by a factor of 2.

The left part of Figure 7 shows the first of 30 frames of the time-resolved movie showing the wave-front distortion in the boundary layer (no gas injection). To highlight the dynamic component of the wavefront, the average of all 30 frames was subtracted from each frame, and the data have been corrected for spherical aberration caused by the divergence of the incident beam (see Figure 6). In the movie, some evidence of turbulent structures convecting downstream is apparent, as well as significant noise. Turbulent hypersonic boundary layers can have very large relative density fluctuations, on the order of 40% of the average density, but since the average density in the facility was very low, the absolute difference in density is small, resulting in small phase distortions.

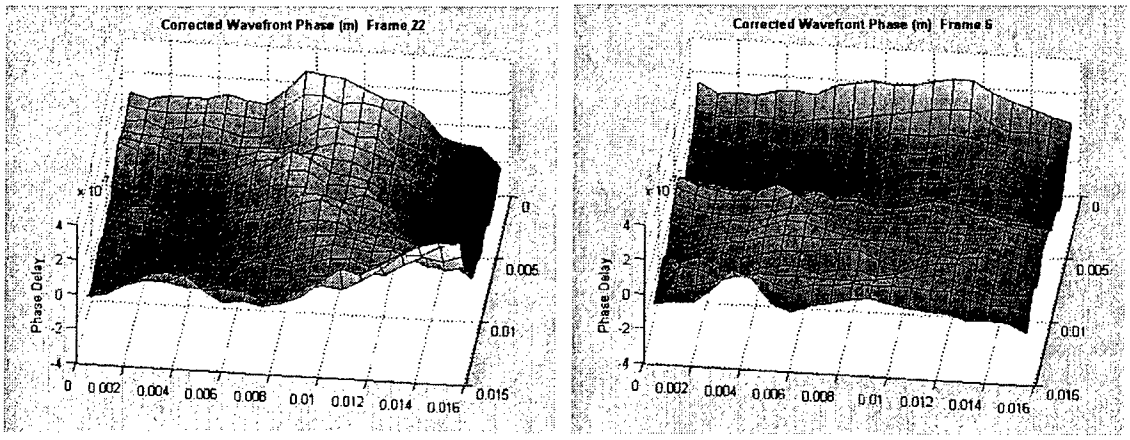

Figure 7: Mach 8 flat plate boundary layer phase front measurements, raw data corrected for spherical aberration. Left: without helium injection. Right: with helium injection (J = 0.12). Flow is from left to right, all axes in meters.

The right part of Figure 7 shows a similar frame from a movie of the phase distortion in a flat plate boundary layer with helium injection. The characteristic influence of the helium is seen through the presence of strong longitudinal features associated with the longitudinal vortical structures.

A full error analysis has been completed, that included an assessment of alternative fitting procedures (non-Gaussian). The assessment showed that Gaussian fits are near optimum. In addition, a number of steps were taken to improve the signal to noise ratio by altering the focal ratio of the 4f lens system, and current signal-to-noise ratios are about 2.6. Error estimates for the Mach 8 boundary layer experiments are shown in Figure 8 for the no injection case, and in Figure 9 for the case with injection. Further analysis is continuing.

We have also been able to significantly improve our data analysis software. The software now computes the x and y uncertainty for each centroid fit on each spot in the image. These uncertainties are then propagated through to the uncertainty on x and y phase slopes, and these are used to weight the least squares fit of the biquadratic phase surface. This will not only improve the quality of the fit, it also allow the uncertainty on each pixel to be propagated all the way through to an uncertainty on the final phase surface.

4. Subsonic Results

Our initial efforts were all performed at the higher Mach number to allow extensive tests on the sensor performance, the data analysis, and the analysis of the errors and uncertainties. In all respects, however, the basic design and operation of this high Mach number sensor is also suitable for subsonic applications. Furthermore, the model used to generate the flat plate boundary layer at Mach 8, and indeed the working section itself, could be used for the subsonic study with only minor modifications (Figure 6).

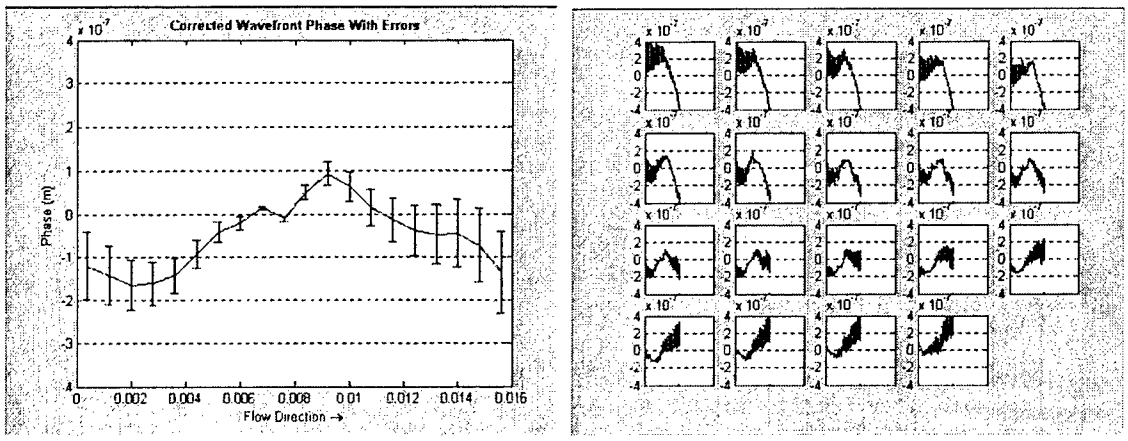

Figure 8: Error analysis corresponding to phase measurements shown in Figure 7, no injection. Left: single streamwise slice. Right: all streamwise slices.

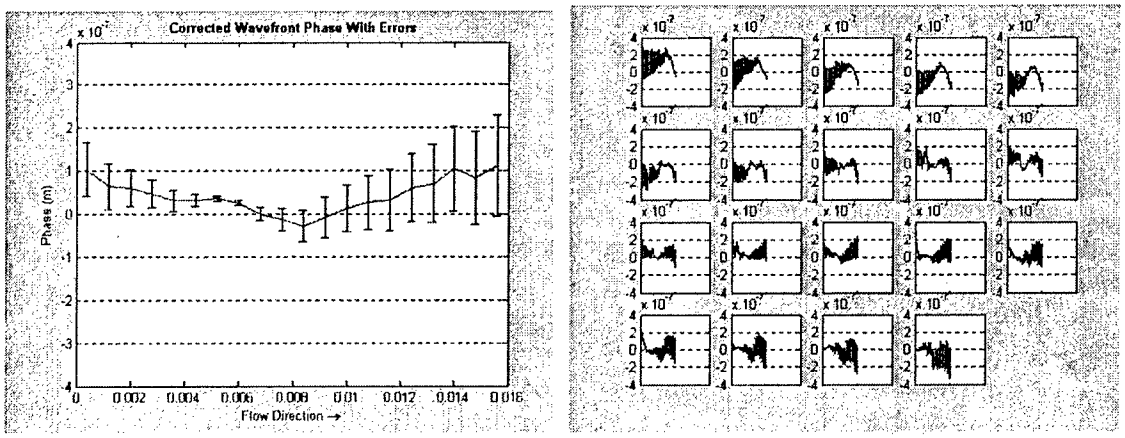

Figure 9: Error analysis corresponding to phase measurements shown in Figure 7, with injection. Left: single streamwise slice. Right: all streamwise slices.

To adapt the high Mach number Shack-Hartmann sensor for subsonic applications, a new Redlake HGLE high speed digital CMOS camera was acquired with resolutions ranging from 752 x 1128 pixels at 1000 fps, 512 x 512 at 2000 fps, and 256 x 256 at 5000 fps. The camera was funded through a related SBIR program with ISSI under the direction of Sivaram Gogineni. The camera is capable of a "line" resolution mode, 20 x 1128 pixels at 50,000 fps, which is particularly useful for comparing Shack-Hartmann data to Malley probe data. The resolution of this camera is much better than the Princeton Scientific camera (180 x 180 pixels), it has a lower noise level, and the pixel size is much smaller, all factors that allow a more precise definition of spot size and movement. This is necessary for flows where the density fluctuations are relatively weak, as in low subsonic boundary layers.

The Shack-Hartmann wavefront analyzer was then installed in the Princeton Gasdynamics transonic facility (M = 0.6-0.9) and preliminary measurements of aero-optic distortion in the flowfield over a flat plate at Mach 0.65 were obtained using the Redlake camera. The flat plate model and test section and model were the same as that used at the higher Mach

numbers (Figure 6). Figure 10 shows the wavefront distortion with and without helium injection. Although the helium injection momentum ratio (ratio of the jet to freestream momentum flux) is matched between the hypersonic and transonic cases, we no longer see stable longitudinal structures in the injection case. We believe this is due to the different Reynolds numbers of the two jets. We will test this hypothesis by varying the slot geometry in the coming months.

Ongoing experiments will quantify the mitigation of aero-optic distortions by comparing the calculated far-field with no injection, with injection and no deformable optics, and with both injection and simulated deformable optics. The shape of these deformable optics will be fixed by the expected average phase distortion and will not be moved in real time. This will replicate the actual flight situation where the optical system will not have the temporal bandwidth required to adapt in real time. Success of the mitigation scheme will be determined by a repeatable increase in the Strehl ratio. The experiments are currently underway, and the results are expected to be available before the end of the calendar year. In addition, the error analysis is now being used to help optimize the sensor performance. It is clear that the choice of lenslet array is a critical parameter, in that the focal length of the lenslets controls the sensitivity of the array, and the number of spots dictates the spatial resolution. There is a trade-off between sensitivity and dynamic range which must be optimized depending on the specific parameters of the flow and optical arrangement. The error analysis is a crucial factor in making optimal design choices.

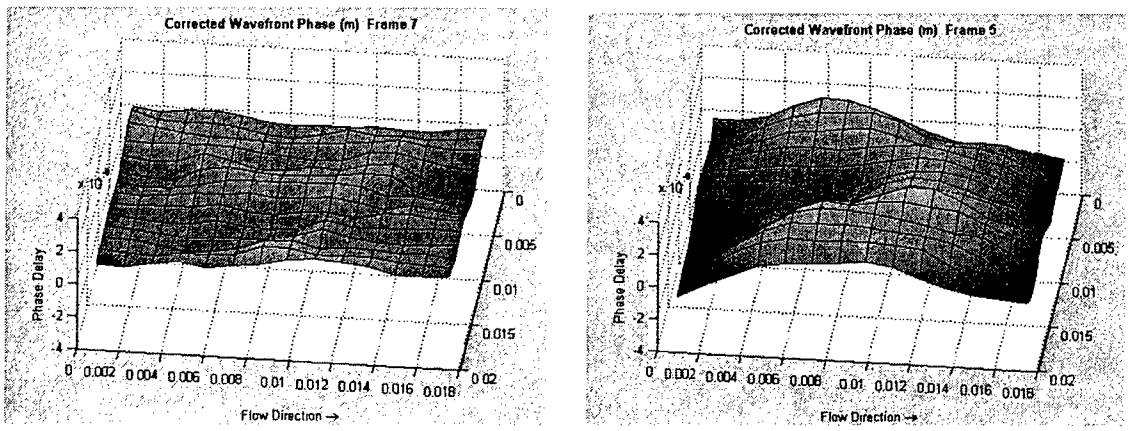

Figure 10: Phase front distortion in a Mach 0.65 boundary layer. All axes are in meters. Flow is from left to right. Left: without helium injection; Right: with helium injection.

Finally, we intend to make direct comparisons between Shack-Hartmann data and Malley probe data on OPD by obtaining fully-resolved data sets using the Redlake camera in the "line" mode (20 x 1128 pixels at 50,000 fps).

5. Summary

To summarize, our efforts to date have yielded:

1. A MHZ-rate Shack-Hartmann sensor capable of real-time measurements of two-dimensional wavefront distortion in hypersonic and subsonic turbulent boundary layers;
2. A kHz-rate two-dimensional Shack-Hartmann sensor adapted for high subsonic turbulent boundary layers to obtain higher sensitivity and resolution;
3. An extensive software suite for analysing Shack-Hartmann data;
4. A full error analysis for Shack-Hartmann applications, that is a vital design component for constructing optimal sensors.
5. A complete data set on wavefront distortion in a flat plate turbulent boundary layer at Mach numbers of 0.65 and 8, with and without the injection of helium for purposes of controlling wavefront distortion.

In the next few months, we intend to:

1. Derive far-field Strehl ratios for the flat plate turbulent boundary layer at Mach numbers of 0.65 and 8, with and without the injection of helium;
2. Assess the efficacy of helium injection for control purposes;
3. Make direct comparisons between Shack-Hartmann data and Malley probe data on OPD measurement.

Acknowledgment/Disclaimer

This work was sponsored (in part) by the Air Force Office of Scientific Research, USAF, under grant/contract number F49620-02-1-0124. The views and conclusions contained herein are those of the authors and should not be interpreted as necessarily representing the official policies or endorsements, either expressed or implied, of the Air Force Office of Scientific Research or the U.S. Government.

References

Auvity, B., Etz, M., Huntley, M., Pingfan Wu and Smits, A.J. "Control of Hypersonic Boundary Layers by Helium Injection," AIAA Paper 2000-2322, Fluids 2000 Conference, Denver, Colorado, June 19-22, 2000.

Auvity, B., Etz, M. R. and Smits, A. J., "Effects of transverse helium injection on hypersonic boundary layers," Physics of Fluids, V 13, No. 10, Oct. 2001.

Cicchiello, J. M. and Jumper, E. J., "Far-Field Optical Degradation Due to Near-Field Transmission Through a Turbulent Heated Jet," Applied Optics, Vol. 36, No. 25, 1997.

Erbland, P.J., Etz, M.R., Lempert, W.R., Smits, A.J. and Miles, R. B. "Optical refraction from high Mach number turbulent boundary layer structures," AIAA Paper 98-0399, 36th Aerospace Sciences Meeting, January 12-15, 1998, Reno, NV.

Fitzgerald E. J. and Jumper, E. J., "Further Consideration of Compressibility Effects on Shear Layer Optical Distortion," AIAA Paper 99-3617, 1999.

Fitzgerald E. J. and Jumper, E. J., "Extension of the Small-Aperture Beam Technique to the Measurement of Full, 2-Dimensional Optical Wavefronts," SPIE Paper 3172-11, Proceedings of the Optical Technology in Fluid, Thermal, and Combustion Flow III, SPIE-The International Society of Optical Engineering, 1997.

Gad-el-Hak, M., "Modern Developments in Flow Control", Applied Mechanics Reviews, Vol. 49, pp. 365-379, 1996.

Ho, C. H., and Tai, Y. C., "Review: MEMS and its Applications for Flow Control," ASME Journal of Fluids Engineering, Vol. 118, September 1996.

Huntley, M. B., Wu, P., Miles, R. B. and Smits, A. J., "MHz Rate Imaging of Boundary Layer Transition on Elliptic Cones at Mach 8," AIAA Paper 00-0379, Proceedings of 38th Aerospace Sciences Meeting and Exhibit, 2000.

Jumper E. J. and Fitzgerald, E. J., "Recent advances in aero-optics," Progress in Aerospace Sciences 37, 299–339, 2001

McMichael, J. M., "Progress and Prospects for Active Flow Control Using Microfabricated ElectroMechanical Systems (MEMS)," AIAA Paper 96-0306, January 1996.

Moin, P., Wang, M. and Mani, A., "Computational study of aero-optical distortion by turbulent wake," AFOSR 2004 Contractors' Meeting in Turbulence and Rotating Flows, Denver CO, August 4-5, 2004.

Rowley, C.W. and D.R. Williams, "Control of forced and self-sustained oscillations in the flow past a cavity." AIAA paper 2003-0008, 41st AIAA Aerospace Sciences Meeting, January 2003.

Southwell, W. H., "Wavefront Estimation from Wavefront Slope Measurements," Journal of the Optical Society of America, Vol. 70, No. 8, 998-1006, 1980.

Stanek, M. J., Raman, G., Kibens, V., Ross, J. A., Jessaji, O. and Peto, J. W., "Control of Cavity Resonance Through Very High Frequency Forcing," AIAA Paper 2000-1905, 6th AIAA/CEAS Aeroacoustics Conference, June 2000.

Stanek, M. J., Sinha, N., Seiner, J. M., Pearce, B. and Jones, M. I., "High Frequency Flow Control - Suppression of Aero-Optics In Tactical Directed Energy Beam Propagation & The Birth of a New Model (Part I)," AIAA 2002-2272, 33rd AIAA Plasmadynamics & Lasers Conference, May 2002.

Thurow, B., Samimy, M. and Lempert, W., "Simultaneous MHz Rate Flow Visualization and Wavefront Sensing for Aero-Optics," AIAA Paper 2003-0684, Proceedings of 38th Aerospace Sciences Meeting and Exhibit, 2003.

Wyckham, C. M., Zaidi, S. H., Miles, R. B. and Smits A. J. "Characterization of Optical Wavefront Distortions due to a Boundary Layer at Hypersonic Speeds," AIAA Paper 2003-4308, 34th AIAA Plasmadynamics and Lasers Conference, 23-26 June 2003, Orlando, Florida.

Zaidi, S.H., Shneider, M.N., Mansfield, D.K., Ionikh, Y.Z. and Miles, R.B. "Influence of Upstream Pulsed Energy Deposition on a Shockwave Structure in Supersonic Flow," AIAA Paper 2002-2703, Proceedings of 22nd AIAA Aerodynamics Measurement Technology and Ground Testing Conference, 2002.

Personnel Supported

Phillip Kang	Undergraduate student, Princeton University, Princeton, NJ
Chris Wyckham	Graduate Student, Princeton University, Princeton NJ
S.H. Zaidi	Research Staff Member, Princeton University, Princeton NJ
Alexander J. Smits	Professor, Princeton University, Princeton NJ
Richard B. Miles	Professor, Princeton University, Princeton NJ

Publications acknowledging this grant

1. Auvity, B., Etz, M.R. and Smits, A.J. "Effects of Transverse Helium Injection on Hypersonic Boundary Layers." Physics of Fluids, Vol. 13(10), pp. 3025-32, 2001
2. Wyckham, C. M., Zaidi, S. H., Miles, R. B. and Smits A. J. "Characterization of Optical Wavefront Distortions due to a Boundary Layer at Hypersonic Speeds," AIAA Paper 2003-4308, 34th AIAA Plasmadynamics and Lasers Conference, 23-26 June 2003, Orlando, Florida.
3. Wyckham, C. M., Zaidi, S. H., Miles, R. B. and Smits, A. J., "Measurement of Aero-Optic Distortion Due to Hypersonic, Turbulent Boundary Layers With Gas Injection" AIAA Paper 2005-XXXX, 35th AIAA Fluid Dynamics Conference, 6-9 June 2005, Toronto, Ontario, Canada.
4. Bookey, P. Wyckham, C. M. and Smits A. J., "Experimental Investigations of Mach 3 Shock-Wave Turbulent Boundary Layer Interactions," AIAA Paper 2005-XXXX, 35th AIAA Fluid Dynamics Conference, 6-9 June 2005, Toronto, Ontario, Canada.

5. Chris Wyckham, Sohail Zaidi, Richard Miles and Alexander Smits, "Developing a MHz Rate Wavefront Sensor for Characterization of Aero-Optic Distortion in a Hypersonic, Turbulent Boundary Layer," Paper #EF06, 55th Meeting of the American Physical Society Division of Fluid Dynamics, East Rutherford, NJ, November 23-25, 2003.
6. Christopher Wyckham, Richard Miles, Alexander Smits and Sivaram Gogineni, "Flow control for enhanced aero-optic performance in turbulent boundary layers," Paper #DB008, 56th Meeting of the American Physical Society Division of Fluid Dynamics, Seattle, WA, November 21-23, 2004.

Awards Received

APS Fellow—awarded November 1997 (A.J. Smits)
AIAA Aerodynamic Measurement Technology Award—January 2000 (R.B. Miles)
AIAA Fellow—awarded April 2000 (R.B. Miles), April 2002 (A.J. Smits)
RAeS Fellow—awarded January 2002 (A.J. Smits)